AIAA JOURNAL
Vol. 47, No. 4, April 2009

Joint Uncertainty Propagation in Linear Structural Dynamics Using Stochastic Reduced Basis Methods

F. Dohnal,* B. R. Mace,† and N. S. Ferguson‡
University of Southampton, Highfield, Southampton SO17 1BJ, United Kingdom

DOI: 10.2514/1.38974

Uncertainties in the properties of joints produce uncertainties in the dynamic response of built-up structures. Line joints, such as glued or continuously welded joints, have spatially distributed uncertainty and can be modeled by a discretized random field. Techniques such as Monte Carlo simulation can be applied to estimate the output statistics, but computational cost can be prohibitive. This paper addresses how uncertainties in joints might be included straightforwardly in a finite element model, with particular reference to approaches based on fixed-interface (Craig–Bampton) component mode synthesis and a stochastic reduced basis method with two variants. These methods are used to determine the output statistics of a structure. Unlike perturbation-based methods, good accuracy can be achieved even when the coefficients of variation of the input random variables are not small. Undamped as well as proportionally damped components are considered. Efficient implementations are proposed based on an exact matrix identity that leads to a significantly lower computational cost if the number of joint degrees of freedom is sufficiently small compared with the structure's overall number of degrees of freedom. A numerical example is presented. The proposed formulation is an efficient and effective implementation of a stochastic reduced basis projection scheme. It is seen that the method can be up to orders of magnitude faster than direct Monte Carlo simulation, while providing results of comparable accuracy. Furthermore, the proposed implementation is more efficient when fewer joints are affected by uncertainty.

I. Introduction

WHEN constructing numerical models of real-life engineering systems, it is often assumed that the system under consideration is deterministic. In practice, however, some degree of uncertainty in the system properties and operating environment is inevitable (e.g., boundary conditions, material properties, etc.). In such situations, an individual deterministic realization of the system properties and the environmental conditions might be undesirable, because this could lead to misleading response predictions. A commonly used approach in engineering design is to introduce safety factors to indirectly account for parameter uncertainty. However, this approach typically leads to highly conservative designs and may not be appropriate for new lightweight materials and novel design concepts.

With continuous growth in computing power and recent development of sophisticated numerical techniques, reliable numerical simulations of systems with uncertainty can be obtained by quantifying input uncertainties to the model equations and propagating them to the system response numerically. In contrast to deterministic analysis, which only provides response predictions at a single point in the ensemble corresponding to the nominal values of the system parameters, this approach provides a range of response values, which can be valuable in the design process.

Simulation techniques commonly used, such as direct Monte Carlo simulation (MCS), can be applied to approximate the output statistics to an arbitrary degree of accuracy, provided that a sufficient number of samples is used. Unfortunately, the computational cost of direct simulation techniques can be prohibitive for large-scale models. There are three main approaches to reduce the computational cost of large models: 1) advanced Monte Carlo methods [1–6] (e.g., importance sampling, line sampling, etc.), 2) perturbation-based methods [7–9], and (3) stochastic finite element methods [10–13]. The latter techniques offer computationally efficient alternatives to MCS and have been widely applied to approximate the first two statistical moments of the system response. Unlike perturbation-based methods, stochastic finite element methods, for example, the stochastic reduced basis method (SRBM) [14], can achieve good accuracy even when the coefficients of variation of the random variables are large.

There are typically uncertainties in the properties of joints in mechanical structures (e.g., bolts, rivets, spot welds, glue, etc.), which subsequently produce uncertainties in the dynamic response of built-up structures. The influence of uncertainty in joints on the resulting response of the whole structure is often analyzed by MCS based on finite element (FE) analysis of meshed structures. In general, the computational cost is quite high. Therefore, component mode synthesis (CMS) may be performed in order to reduce the size of the model, which has benefits for repeated calculations. This method is based on eigendecomposition of the stiffness and mass matrices leading to a reduced size of the model. The approach offers a straightforward, intuitive way of describing uncertainty in structures built up from substructures, because the properties of the individual substructures and joints can be included in a clear manner.

This paper addresses how uncertainties in joints might be included straightforwardly in a finite element model of a structure, with particular reference to approaches based on fixed-interface (Craig–Bampton) CMS, see [15,16]. The spatially distributed uncertainty in the joints is modeled by a discretized random field [17–19]. As proposed here, the efficiency of the SRBM [14] can be enhanced further in two steps by combination with CMS and matrix algebra. The former approach truncates the number of degrees of freedom for each component separately, whereas the latter reduces the global stochastic algebraic equation to a much smaller size, the size being the number of joint degrees of freedom, instead of retaining all of the system degrees of freedom.

In general, the presence of damping in the system gives rise to complex modes. For proportional or Rayleigh damping (i.e., damping proportional to mass and/or stiffness matrices) the undamped modes are also modes of the damped system, and damping

Received 6 June 2008; revision received 9 December 2008; accepted for publication 15 December 2008. Copyright © 2009 by the American Institute of Aeronautics and Astronautics, Inc. All rights reserved. Copies of this paper may be made for personal or internal use, on condition that the copier pay the $10.00 per-copy fee to the Copyright Clearance Center, Inc., 222 Rosewood Drive, Danvers, MA 01923; include the code 0001-1452/09 $10.00 in correspondence with the CCC.

*Post-Doctoral Researcher, Institute of Sound and Vibration Research.
†Professor of Structural Dynamics, Institute of Sound and Vibration Research.
‡Senior Lecturer in Structural Dynamics, Institute of Sound and Vibration Research.

can be included straightforwardly by ascribing a loss factor η to each mode. In practice, the effects of nonproportional damping are often small, and, as in this paper, damping is assumed to be proportional.

In the next section, CMS of undamped system components is briefly reviewed with a focus on the fixed-interface approach. Subsequently, the modelling of joints with spatial correlation in terms of a random field is described. The calculation of system response statistics by direct MCS with CMS and SRBM with CMS is presented. Finally, the proposed methods are benchmarked on a numerical example to illustrate the efficiency and accuracy of the proposed procedures. This paper represents a summary and extension of the works presented in [20,21].

II. Component Mode Synthesis

CMS is a technique that can reduce the size of the system matrices of built-up structures, in order to reduce the computational cost of the dynamic response calculation. The systems under considerations are assumed to be built up from a number of connected subsystems. In this paper, the subsystems are modeled with respect to their local modes. At this component level the undamped substructure is represented by an FE model that can be written in the form

$$\mathbf{M}^{(s)}\ddot{\mathbf{x}}^{(s)} + \mathbf{K}^{(s)}\mathbf{x}^{(s)} = \mathbf{f}^{(s)} \tag{1}$$

where $\mathbf{M}^{(s)}$ and $\mathbf{K}^{(s)}$ are the $n^s \times n^s$ mass and stiffness matrices, $\mathbf{x}^{(s)}$ and $\mathbf{f}^{(s)}$ are the $n^s \times 1$ vectors of physical displacement coordinates and external forces acting on the substructure/component s, and n^s is their total number of degrees of freedom. The superscript (s) will be omitted for the rest of this section.

The displacement coordinates $\mathbf{x}$ are partitioned into n_i^s interior (i) and n_b^s boundary (b) coordinates, where $n = n_i^s + n_b^s$. Equation (1) yields

$$\begin{bmatrix} \mathbf{M}_{ii} & \mathbf{M}_{ib} \\ \mathbf{M}_{bi} & \mathbf{M}_{bb} \end{bmatrix} \begin{bmatrix} \ddot{\mathbf{x}}_i \\ \ddot{\mathbf{x}}_b \end{bmatrix} + \begin{bmatrix} \mathbf{K}_{ii} & \mathbf{K}_{ib} \\ \mathbf{K}_{bi} & \mathbf{K}_{bb} \end{bmatrix} \begin{bmatrix} \mathbf{x}_i \\ \mathbf{x}_b \end{bmatrix} = \begin{bmatrix} \mathbf{f}_i \\ \mathbf{f}_b \end{bmatrix} \tag{2}$$

Because for a purely mechanical structure the system matrices are symmetric, the relations $\mathbf{M}_{ib} = \mathbf{M}_{bi}^T$ and $\mathbf{K}_{ib} = \mathbf{K}_{bi}^T$ hold, where T denotes the transpose. Different CMS methods exist for reducing the size of the system matrices, for example [15,16,22]. Here, the Craig–Bampton method [16], outlined in the subsequent section, is followed, although other methods are applicable within this framework.

A. Craig–Bampton Procedure

This method uses the normal modes of the components with the boundary coordinates fixed in combination with static constraint modes. The fixed-interface normal modes of a single component are the natural modes of the component with all boundary coordinates fixed, given by the right-eigenvalue problem

$$\mathbf{K}_{ii}\boldsymbol{\phi}_l = \omega_l^2 \mathbf{M}_{ii}\boldsymbol{\phi}_l \tag{3}$$

Here, the n_i eigenfrequencies ω_l are those of the of the fixed component and the corresponding eigenvectors $\boldsymbol{\phi}_l$ are mass normalized so that

$$\boldsymbol{\phi}_k^T \mathbf{M}_{ii}\boldsymbol{\phi}_l = \delta_{kl}, \qquad \boldsymbol{\phi}_k^T \mathbf{K}_{ii}\boldsymbol{\phi}_l = \omega_l^2 \delta_{kl}, \qquad k, l = 1, 2, \ldots, n_i \tag{4}$$

where δ_{kl} is the Kronecker delta. The modal matrix with respect to all component modal coordinates $\mathbf{q} = [\mathbf{q}_i^T, \mathbf{q}_b^T]^T$ is composed from these n_i^s Ritz vectors as

$$\boldsymbol{\Phi} = \begin{bmatrix} \phi_1 & \phi_2 & \cdots & \phi_{n_i} \\ \mathbf{0} & \mathbf{0} & \cdots & \mathbf{0} \end{bmatrix} = \begin{bmatrix} \boldsymbol{\Phi}_i \\ \mathbf{0} \end{bmatrix} \tag{5}$$

This set of modes is complemented by a set of n_b^s static constraint modes. Together they form a linearly independent set. The static constraint modes chosen are the static displacements of a component due to unit displacement of a single boundary coordinate while keeping all other boundary coordinates fixed. The matrix of constraint modes is defined by

$$\boldsymbol{\Psi} = \begin{bmatrix} -\mathbf{K}_{ii}^{-1}\mathbf{K}_{ib} \\ \mathbf{I}_{bb} \end{bmatrix} = \begin{bmatrix} \boldsymbol{\Psi}_i \\ \mathbf{I}_{bb} \end{bmatrix} \tag{6}$$

where the upper part corresponds to a Guyan reduction [23]. The matrices in Eqs. (5) and (6) define a transformation of the physical coordinates $\mathbf{x}$ to component modal coordinates $\mathbf{q}$ defined by

$$\begin{bmatrix} \mathbf{x}_i \\ \mathbf{x}_b \end{bmatrix} = \mathbf{B}\begin{bmatrix} \mathbf{q}_i \\ \mathbf{q}_b \end{bmatrix}, \qquad \mathbf{B} = \begin{bmatrix} \boldsymbol{\Phi} & \boldsymbol{\Psi} \end{bmatrix} \tag{7}$$

where the coefficient matrix $\mathbf{B}$ is of size $(n_i^s + n_b^s) \times (n_i^s + n_b^s)$. A reduction in the size of the component matrices is achieved by retaining only some of the fixed-interface normal modes, that is, those with the lowest eigenfrequencies. If only the first n_k^s modes are kept (with $n_k^s \ll n_i^s$) the coordinate vector $\mathbf{q}_i$ is replaced by $\mathbf{q}_k$, and the transformation in Eq. (7) is approximated by

$$\mathbf{B}_k = \begin{bmatrix} \boldsymbol{\Phi}_k & \boldsymbol{\Psi} \end{bmatrix} \tag{8}$$

where $\boldsymbol{\Phi}_k$ is the matrix of kept mode shapes. Applying this transformation, the component matrices reduce to

$$\mathbf{M}_k = \mathbf{B}_k^T \mathbf{M} \mathbf{B}_k, \qquad \mathbf{K}_k = \mathbf{B}_k^T \mathbf{K} \mathbf{B}_k, \qquad \mathbf{f}_k = \mathbf{B}_k^T \mathbf{f} \tag{9}$$

leading to the undamped modal system of the component of size $n_r^s = n_k^s + n_b^s$

$$\begin{bmatrix} \mathbf{I}_{kk} & \mathbf{M}_{kc} \\ \mathbf{M}_{kc}^T & \mathbf{M}_{cc} \end{bmatrix} \begin{bmatrix} \ddot{\mathbf{q}}_k \\ \ddot{\mathbf{q}}_b \end{bmatrix} + \begin{bmatrix} \boldsymbol{\Lambda}_{kk} & \mathbf{0} \\ \mathbf{0} & \mathbf{K}_{cc} \end{bmatrix} \begin{bmatrix} \mathbf{q}_k \\ \mathbf{q}_b \end{bmatrix} = \begin{bmatrix} \mathbf{f}_k \\ \mathbf{f}_b \end{bmatrix} \tag{10}$$

where $\boldsymbol{\Lambda}_{kk}$ is a diagonal matrix of the eigenvalues ω_k^2. The submatrices in Eq. (10) are expressed explicitly as

$$\begin{aligned} \mathbf{K}_{cc} &= \mathbf{K}_{bb} + \mathbf{K}_{bi}^T \boldsymbol{\Psi}_i, \qquad \mathbf{M}_{kc} = \boldsymbol{\Phi}_k^T (\mathbf{M}_{ib} + \mathbf{M}_{ii}\boldsymbol{\Psi}_i) \\ \mathbf{M}_{cc} &= \mathbf{M}_{bb} + \mathbf{M}_{bi}^T \boldsymbol{\Psi}_i + \boldsymbol{\Psi}_i^T \mathbf{M}_{ib} + \boldsymbol{\Psi}_i^T \mathbf{M}_{ii} \boldsymbol{\Psi}_i \end{aligned} \tag{11}$$

B. Synthesis of Undamped Components

After the reduction at the component level, the components are assembled into global system matrices of reduced size. First, the system matrices of the components are arranged in global system matrices of size $\sum_s (n_k^s + n_b^s)$

$$\mathbf{A}_d = \operatorname{diag}(\mathbf{A}_k^{(1)}, \ldots, \mathbf{A}_k^{(c)}), \qquad \mathbf{f}_d = [\mathbf{f}_k^{(1),T}, \ldots, \mathbf{f}_k^{(c),T}]^T \tag{12}$$

with respect to the vector of all component coordinates

$$\mathbf{q} = [\mathbf{q}_k^{(1),T}, \mathbf{q}_b^{(1),T}, \ldots, \mathbf{q}_k^{(c),T}, \mathbf{q}_b^{(c),T}]^T \tag{13}$$

where c is the number of components and $\mathbf{A}^{(i)}$ is the mass or stiffness matrix, $\mathbf{M}^{(i)}$ or $\mathbf{K}^{(i)}$, as defined in Eq. (10). The components are coupled by enforcing displacement continuity along the interface coordinates of two components s and p

$$\mathbf{x}_b^{(s)} = \mathbf{x}_b^{(p)} \quad \text{or} \quad \text{equivalently } \mathbf{q}_b^{(s)} = \mathbf{q}_b^{(p)} \tag{14}$$

leading to linearly dependent global matrices in Eq. (12). A transformation between the linearly dependent component modal coordinates $\mathbf{q}$ and the linearly independent set of global component coordinates $\mathbf{u}$ is introduced

$$\mathbf{q} = \mathbf{S}\mathbf{u} = \begin{bmatrix} \mathbf{I}_{ii} & \mathbf{0}_{ib} \\ & \mathbf{D} \end{bmatrix} \begin{bmatrix} \mathbf{u}_i \\ \mathbf{u}_b \end{bmatrix} \tag{15}$$

where $\mathbf{D}$ is defined by the relations in Eq. (14). Because only interface coordinates are related in Eq. (14), the interior coordinates are not affected by this transformation. The coefficient matrix $\mathbf{S}$ is of size $(n_b + \sum_s n_k^s) \times (n_b + \sum_s n_k^s)$, where $n_b < \sum_s n_b^s$ is the number of linearly independent interface degrees of freedom. Finally, the

global system matrices with respect to the global component coordinates $\mathbf{u}$ are

$$\mathbf{A} = \mathbf{S}^T \mathbf{A}_d \mathbf{S}, \qquad \mathbf{f} = \mathbf{S}^T \mathbf{f}_d \tag{16}$$

leading to the global undamped system of size $n_r = n_b + \sum_s n_k^s$

$$\begin{bmatrix} \mathbf{I}_{kk} & \mathbf{M}_{kc} \\ \mathbf{M}_{kc}^T & \mathbf{M}_{cc} \end{bmatrix} \begin{bmatrix} \ddot{\mathbf{u}}_i \\ \ddot{\mathbf{u}}_b \end{bmatrix} + \begin{bmatrix} \mathbf{\Lambda}_{kk} & \mathbf{0} \\ \mathbf{0} & \mathbf{K}_{cc} \end{bmatrix} \begin{bmatrix} \mathbf{u}_i \\ \mathbf{u}_b \end{bmatrix} = \begin{bmatrix} \mathbf{f}_i \\ \mathbf{f}_b \end{bmatrix} \tag{17}$$

C. Damping

Real-life components possess some kind of energy dissipation mechanism or damping. In general, engineering structures are damped nonproportionally, in which case the undamped modes are coupled through off-diagonal terms in the modal damping matrix, and, consequently, the system possesses complex modes instead of real ones.

Here, proportional damping, also known as Rayleigh damping, is assumed. For this the damping matrix is a linear combination of the mass and stiffness matrices

$$\mathbf{C} = \beta_1 \mathbf{M} + \beta_2 \mathbf{K} \tag{18}$$

where β_1 and β_2 are scalars. For this special type of damping the equations of motion, when transformed to the undamped modes, become uncoupled. Each mode i is then associated with a loss factor η_i, which might vary from one mode to the next.

III. Modelling Uncertainty in Joints

Uncertainty and variability in the description of real-life engineering systems are unavoidable. In this paper the effects of uncertainties are considered for the particular case of uncertainties in joints, and especially in line joints (e.g., continuously welded or glued joints).

A spatial correlation of a line joint property is introduced and modeled as a one-dimensional random field defined by a correlation function $R\{r; a, \sigma\}$, where σ^2 is the variance, r is the distance between two points in the joint, and a is the correlation length. The field is homogeneous because its value depends only on the distance between two positions. In a practical application determining this function might be difficult. In the numerical example the specific correlation function

$$R\{r; a, \sigma\} = \sigma^2 \exp\left\{-\frac{|r|}{a}\right\} \tag{19}$$

is used to represent uncertainty in a physical parameter. Assuming an exponential dependency means that adjacent values of the uncertain parameter do not differ, on average, as much as values that are further apart. For small values of a, the discretized covariance matrix is close to a diagonal matrix leading to weak correlation in space. For large values of a, this matrix becomes almost fully occupied and the correlation is strong.

Various discretization techniques are available in the literature for approximating continuous random fields [18,19]. The emphasis of this paper is the Karhunen–Loève expansion [12,17] of a real, scalar random field p as

$$p\{r, \vartheta\} = \langle p\{r\} \rangle + \sum_{i=1}^{\infty} \sqrt{\lambda_i}\, \kappa_i\{r\} \xi_i\{\vartheta\} \tag{20}$$

where ϑ is a parameter for the random subspace, $\langle \cdot \rangle$ denotes the expectation operator (mean value), and $\xi_i\{\vartheta\}$ is a set of (uncorrelated) Gaussian variables with zero mean and unity standard deviation. λ_i and $\kappa_i\{r\}$ are the eigenvalues and eigenfunctions of the integral eigenvalue problem

$$\int R\{r, r'\} \kappa_i\{r\} \mathrm{d}r = \lambda_i \kappa_i\{r'\} \tag{21}$$

where R is the correlation function of the random field p, for example, as defined in Eq. (19). The continuous correlation function is discretized spatially at the finite element coordinates of the joints. Consequently, the previous eigenvalue problem is discretized on the mesh and solved algebraically. In the context of finite elements, the expansion in Eq. (20) is truncated at the mth term leading to a finite dimensional approximation of the random field. The discretized correlation function yields a covariance matrix, for which the Karhunen–Loève expansion (or equivalently a polynomial chaos approximation of first order, see [12]) can be applied to model a spatially correlated physical property d as

$$d\{\vartheta\} = \langle d\{\vartheta\} \rangle + \sum_{r=1}^{m} \sqrt{\lambda_r}\, \chi_r \xi_r\{\vartheta\} \tag{22}$$

where λ_r and χ_r are the eigenvalues and eigenvectors of the covariance matrix. This expansion technique allows random fields to be approximated in terms of a finite set of random variables.

In the subsequent study only the stiffness matrix of the joint is considered to be uncertain. However, it is straightforward to adapt the procedure to an arbitrary joint with uncertain stiffness and/or mass matrices. If the continuous joint is treated as a single component in the CMS model, its stiffness matrix can be written as

$$\mathbf{K}^{(j)}\{\vartheta\} = \langle \mathbf{K}^{(j)}\{\vartheta\} \rangle + \sum_{r=1}^{m} \mathbf{K}_r^{(j)} \xi_r\{\vartheta\} \tag{23}$$

where $\langle \mathbf{K}^{(j)}\{\vartheta\} \rangle$ and $\mathbf{K}_r^{(j)}$ are deterministic component matrices, according to Eq. (22). Ascribing the damping matrix in Eq. (18), the nondeterministic counterpart of the deterministic equations of motion of the assembled system in Eq. (17) become

$$\mathbf{M}(\ddot{\mathbf{u}} + \beta_1 \dot{\mathbf{u}}) + \left(\langle \mathbf{K}\{\vartheta\} \rangle + \sum_{r=1}^{m} \mathbf{K}_r \xi_r\{\vartheta\} \right) (\mathbf{u} + \beta_2 \dot{\mathbf{u}}) = \mathbf{f} \tag{24}$$

which has the size $n_r = n_b + \sum_s n_k^s$.

Equation (23) is written in terms of a truncated sum of weighted Gaussian variables. This is strictly possible for the homogeneous random field introduced in Eq. (19), which is in the focus of the present study. It should be pointed out that in principal it is only required that the random variables ξ_r are *orthogonal*. For example, when discretizing the elastic modulus (which must physically be positive) it is common to truncate the Gaussian distribution to enforce this condition. For orthogonal random variables, an expansion similar to Eq. (20) holds and the system matrices of a linear system can be written in the form of Eq. (23) but now as a truncated sum of weighted orthogonal random variables. In some cases, non-Gaussian but orthogonal variables or stochastic processes can be approximated by a polynomial chaos expansion (e.g., [24]). If so they can be treated by the proposed procedure as long as the approximation in Eq. (23) is reasonable.

A. Monte Carlo Simulation

MCS is a widely used numerical method for calculating the statistics of a system's response for nondeterministic system properties. For numerical calculations only a fraction of all possible samples taken as sets from the complete space of possible configurations is considered, at which the system model is evaluated repeatedly. According to Eq. (23), each sample consists of a set of m random numbers $\xi_r\{\vartheta\}$. The accuracy of the method depends highly on the number of samples considered. If the number of samples is large enough, indicated by the coefficient of variation of the Monte Carlo estimate, convergence toward the correct statistics is guaranteed. However, with an increasing number of samples the simulation rapidly becomes time consuming. Instead of recalculating the global system matrices for each property sample, the concept of CMS is applied, which has a twofold advantage. First, only the components with nondeterministic parameters need to be evaluated at each sample, whereas the deterministic components are calculated

only once. Second, the dimension of the global system matrices is reduced considerably.

The Ritz vectors in Eq. (8) are recalculated for the non-deterministic joint components by applying Eq. (23) whereas the deterministic components are calculated only once. The reduced component matrices are derived for all components according to Eq. (10). Finally, the system is assembled as in Eq. (17) leading to Eq. (24). For time-harmonic motion at frequency ω, Eq. (24) yields

$$(\mathbf{K}\{\vartheta\}(1 + j\omega\beta_2) - \omega\mathbf{M}(\omega - j\beta_1))\mathbf{u}\{\vartheta;\omega\} = \mathbf{f}\{\omega\} \tag{25}$$

The sum in Eq. (23) is evaluated for each parameter sample ϑ. For a dynamic system response $\mathbf{u}\{\vartheta;\omega\}$, the term in parentheses in Eq. (25) needs to be inverted at every frequency of interest and for each sample. Instead of direct inversion, an acceleration scheme is introduced based on modal decomposition. Solving the undamped global eigenproblem of the fully assembled system

$$\mathbf{K}\{\vartheta\}\mathbf{v}_j = \omega_j^2\mathbf{M}\mathbf{v}_j \tag{26}$$

for each sample these system matrices can be diagonalized to

$$\mathbf{\Lambda}\{\vartheta\} = \mathbf{V}^T\{\vartheta\}\mathbf{K}\{\vartheta\}\mathbf{V}\{\vartheta\}, \qquad \mathbf{I} = \mathbf{V}^T\{\vartheta\}\mathbf{M}\mathbf{V}\{\vartheta\} \tag{27}$$

where the matrix $\mathbf{V}$ consists of real mass-normalized eigenvectors $\mathbf{v}_j$.

The solution to Eq. (25) thus becomes complex in the damped case and real in the undamped case

$$\mathbf{u}\{\vartheta;\omega\} = \mathbf{V}\{\vartheta\}(\mathbf{\Lambda}\{\vartheta\}(1 + j\omega\beta_2) - \omega\mathbf{I}(\omega - j\beta_1))^{-1}\mathbf{V}^T\{\vartheta\}\mathbf{f}\{\omega\} \tag{28}$$

Now only diagonal matrices need to be inverted, which is much faster than inverting the matrix in Eq. (25). For the example system in this paper this corresponds to a reduction of about 33%.

B. Stochastic Reduced Basis Methods

Recently, a stochastic reduced basis method was developed in [14] based on [25] for solving systems of linear random algebraic equations in space and the random dimension as in Eq. (25). In contrast to the classical approach in [12], a set of basis vectors spanning a preconditioned stochastic Krylov subspace is employed to approximate the system response. Subsequent application of the Galerkin scheme leads to a reduced-order deterministic system of equations with a significantly lower computational cost.

Introducing the abbreviation of the damped deterministic baseline system for time-harmonic motion

$$\mathbf{A}\{\omega\} = \langle\mathbf{K}\{\vartheta\}\rangle(1 + j\omega\beta_2) - \omega\mathbf{M}(\omega - j\beta_1) \tag{29}$$

and premultiplying Eq. (25) by $\mathbf{A}^{-1}\{\omega\}$ gives the preconditioned, nonsingular algebraic equation

$$\left(\mathbf{I} + \mathbf{A}^{-1}\{\omega\}\sum_{r=1}^{m}\mathbf{K}_r\xi_r\{\vartheta\}(1 + j\omega\beta_2)\right)\mathbf{u}\{\vartheta;\omega\} = \mathbf{A}^{-1}\{\omega\}\mathbf{f}\{\omega\} \tag{30}$$

Instead of inverting the term in parentheses as in the previous section, the solution for the system response $\mathbf{u}\{\vartheta;\omega\}$ is approximated in the preconditioned Krylov subspace, see [14], by a random polynomial

$$\mathbf{u}\{\vartheta;\omega\} \approx \sum_{j=0}^{p}\alpha_j\{\omega\}\mathbf{u}_j\{\vartheta;\omega\} = \mathbf{U}\{\vartheta;\omega\}\boldsymbol{\alpha}\{\omega\} \tag{31}$$

where α_j are deterministic coefficients and $\mathbf{u}_j$ are recursive stochastic basis vectors that form the columns of $\mathbf{U}$ and are defined as

$$\mathbf{u}_0\{\omega\} = \mathbf{A}\{\omega\}^{-1}\mathbf{f}$$
$$\mathbf{u}_{j+1}\{\vartheta;\omega\} = (1 + j\omega\beta_2)\mathbf{A}\{\omega\}^{-1}\sum_{r=1}^{m}\mathbf{K}_r\xi_r\{\vartheta\}\mathbf{u}_j\{\vartheta;\omega\} \tag{32}$$

The inverse of the complex system matrix in Eq. (29) is calculated by applying an acceleration scheme similar to Eq. (28), but now only the eigenproblem of the deterministic baseline system

$$\langle\mathbf{K}\{\vartheta\}\rangle\mathbf{w}_j = \omega_j^2\mathbf{M}\mathbf{w}_j \tag{33}$$

is solved, leading to the diagonal matrices

$$\mathbf{\Lambda} = \mathbf{W}^T\mathbf{K}\mathbf{W}, \qquad \mathbf{I} = \mathbf{W}^T\mathbf{M}\mathbf{W} \tag{34}$$

Finally, the inverse of the baseline system is given by

$$\mathbf{A}\{\omega\}^{-1} = \mathbf{W}(\mathbf{\Lambda}(1 + j\omega\beta_2) - \omega\mathbf{I}(\omega - j\beta_1))^{-1}\mathbf{W}^T \tag{35}$$

In contrast to Eq. (28), Eq. (35) needs to be calculated only once at each frequency ω. For an undamped analysis Eq. (35) simplifies to

$$\mathbf{A}_0\{\omega\}^{-1} = \mathbf{W}(\mathbf{\Lambda} - \omega^2\mathbf{I})^{-1}\mathbf{W}^T \tag{36}$$

To determine the deterministic coefficients α_j in Eq. (31) a Petrov–Galerkin projection scheme according to [14] is applied, that is

$$\left\langle\mathbf{U}^H\{\vartheta;\omega\}\left(\mathbf{A}\{\omega\} + \sum_{r=1}^{m}\mathbf{K}_r\xi_r\{\vartheta\}(1 + j\omega\beta_2)\right)\mathbf{U}\{\vartheta;\omega\}\right\rangle\alpha\{\omega\} = \langle\mathbf{U}^H\{\vartheta;\omega\}\mathbf{f}\{\omega\}\rangle \tag{37}$$

where the superscript H denotes the Hermitian. This algebraic equation is deterministic and of size p, the number of chosen basis vectors in Eq. (31). The projection scheme guarantees convergence with increasing value of p if the inverse of Eq. (29) exists. For the undamped case the system matrices are real and the Hermitian transpose of $\mathbf{U}$ is replaced by the transpose leading to a Bubnov–Galerkin projection scheme [14].

Because the coefficients α_i in Eq. (37) are deterministic scalars, the first two moments of the system response can be expressed in terms of the statistics of the stochastic basis vectors in Eq. (32). The mean of the system response is given by

$$\langle\mathbf{u}\{\vartheta;\omega\}\rangle = \sum_{j=0}^{p}\alpha_j\langle\mathbf{u}_j\{\vartheta;\omega\}\rangle \tag{38}$$

and the covariance matrix is

$$\operatorname{cov}\{\mathbf{u}\{\vartheta;\omega\},\mathbf{u}\{\vartheta;\omega\}\} = \langle\mathbf{u}\{\vartheta;\omega\}\mathbf{u}^H\{\vartheta;\omega\}\rangle = \sum_{j,k=0}^{p}\alpha_j\alpha_k^*\langle\mathbf{u}_j\{\vartheta;\omega\}\mathbf{u}_k^H\{\vartheta;\omega\}\rangle \tag{39}$$

Because the basis vectors in Eq. (32) are computed recursively the number of multiplications increases rapidly with increasing values of p. However, the basis vectors need never be calculated explicitly because only their moments are of interest in Eqs. (38) and (39). Consequently, the expectation operations can be carried out analytically using the joint statistics of $\xi_r\{\vartheta\}$ (e.g. [12]).

Assuming that the solution can be sufficiently well approximated using only a few stochastic basis vectors implies in practice that the levels of uncertainty should be small or moderate (20% or so), and that large levels of uncertainty cannot be accommodated without an unrealistically large number of vectors. However, for mechanical systems, in general, only two or three [14] basis vectors are needed for accurate approximation to the preconditioned Eq. (30).

C. Enhanced Stochastic Reduced Basis Method 1

The calculation procedures can be optimized further by performing the matrix algebra in a particular way, as proposed in the following. The general form of the Sherman–Morrison–Woodbury matrix identity [26] is

$$(\mathbf{A} + \mathbf{PGQ})^{-1} = \mathbf{A}^{-1} - \mathbf{A}^{-1}\mathbf{P}(\mathbf{G}^{-1} + \mathbf{QA}^{-1}\mathbf{P})^{-1}\mathbf{QA}^{-1} \tag{40}$$

Here $\mathbf{A}$ and $\mathbf{G}$ are square matrices whereas $\mathbf{P}$ and $\mathbf{Q}$ are of rectangular shape. If the inverse of $\mathbf{A}$ is known and if the matrix $\mathbf{G}$ has a much

smaller dimension than $\mathbf{A}$, use of this identity is much more efficient than inverting $\mathbf{A} + \mathbf{PGQ}$ directly. Postmultiplying Eq. (40) by $\mathbf{A}$ yields

$$(\mathbf{I} + \mathbf{A}^{-1}\mathbf{PGQ})^{-1} = \mathbf{I} - \mathbf{A}^{-1}\mathbf{P}(\mathbf{G}^{-1} + \mathbf{QA}^{-1}\mathbf{P})^{-1}\mathbf{Q} \tag{41}$$

Introducing a real rectangular matrix $\mathbf{H}$ that transforms the set of global coordinates $\mathbf{u}$ to the subset of joint coordinates $\mathbf{v}$ that correspond to the nondeterministic component, the nondeterministic part of Eq. (24) can be rewritten as

$$\sum_{r=1}^{m} \mathbf{K}_r \xi_r\{\vartheta\} = \sum_{r=1}^{m} \mathbf{H}^T \mathbf{K}_r^W \mathbf{H} \xi_r\{\vartheta\} = \mathbf{H}^T \mathbf{G}\{\vartheta\}\mathbf{H} \tag{42}$$

where the abbreviation $\mathbf{G}\{\vartheta\} = \sum_r \mathbf{K}_r^W \xi_r\{\vartheta\}$ is introduced. Here the dimension of $\mathbf{K}_r^W$ is the same as the number n_j of joint coordinates, and that of $\mathbf{K}_r$ equals the number of global coordinates. The transformation matrix H is of size $n_j \times n_r$. Usually the number of global system coordinates is much larger than the number of joint coordinates, so that the size of $\mathbf{K}_r^W$ is much smaller than the size of $\mathbf{K}_r$. By applying the transformation Eq. (42) to Eq. (30), the inverse of the term in parentheses in Eq. (30) can be calculated according to Eq. (41) as

$$\begin{aligned}(\mathbf{I} + \mathbf{A}^{-1}\{\omega\}\mathbf{H}^T\mathbf{G}\{\vartheta\}\mathbf{H}(1 + \beta_2 j\omega))^{-1} \\ = \mathbf{I} - \mathbf{A}^{-1}\{\omega\}\mathbf{H}^T((1 + \beta_2 j\omega)^{-1}\mathbf{G}^{-1}\{\vartheta\} \\ + \mathbf{H}\mathbf{A}^{-1}\{\omega\}\mathbf{H}^T)^{-1}\mathbf{H}\end{aligned} \tag{43}$$

The advantage of exploiting the identity is that the inverse of the large system matrix $\mathbf{A}$ is already available from the deterministic eigenanalysis of the system. On the right-hand side of Eq. (43) the inverse of a matrix is still needed but is transformed by $\mathbf{H}$ to a fraction of its original size before inversion. Based on Eq. (43), new recursive stochastic basis vectors $\mathbf{v}_j$ are defined by

$$\mathbf{v}_0\{\omega\} = \mathbf{H}\mathbf{A}^{-1}\{\omega\}\mathbf{f}\{\omega\}, \qquad \mathbf{v}_{j+1}\{\vartheta;\omega\} = \mathbf{B}\{\vartheta;\omega\}\mathbf{v}_j\{\vartheta;\omega\} \tag{44}$$

instead of Eq. (32), with the abbreviation

$$\mathbf{B}\{\vartheta;\omega\} = (1 + \beta_2 j\omega)^{-1}\mathbf{G}^{-1}\{\vartheta\} + \mathbf{H}\mathbf{A}^{-1}\{\omega\}\mathbf{H}^T \tag{45}$$

The set of basis vectors $\mathbf{v}_k$ in Eq. (44) spans a Krylov subspace that lies within the subspace spanned by the basis vectors $\mathbf{u}_k$ in Eq. (32) and, consequently, is of much smaller size. The implementation of Eq. (45) takes more effort but leads to smaller matrix operations compared with the calculations of the originally assembled system in Eq. (32) in the previous section. Finally, the original displacement field $\mathbf{u}$ can be expressed in terms of the reduced displacement field $\mathbf{v}$ as

$$\mathbf{A}\{\omega\}\mathbf{u}\{\vartheta;\omega\} = \mathbf{f}\{\omega\} - \mathbf{H}^T\mathbf{v}\{\vartheta;\omega\} \tag{46}$$

where

$$\mathbf{v}\{\vartheta;\omega\} \approx \sum_{j=1}^{p} \gamma_p \mathbf{v}_p \tag{47}$$

The response statistics are evaluated according to the relations in Eqs. (38) and (39). This method is referred here to as the enhanced stochastic reduced basis method (ESRBM1).

D. Enhanced Stochastic Reduced Basis Method 2

The matrix identity can be used in a second approach to generate stochastic vectors of low dimension by introducing the transformation Eq. (46) directly into Eq. (30). Applying the matrix identity in Eq. (43) to Eq. (30) gives

$$\mathbf{u}\{\vartheta;\omega\} = (\mathbf{I} - \mathbf{A}^{-1}\{\omega\}\mathbf{H}^T\mathbf{B}^{-1}\{\vartheta;\omega\}\mathbf{H})\mathbf{A}^{-1}\{\omega\}\mathbf{f}\{\omega\} \tag{48}$$

with the abbreviation in Eq. (45). Introducing the transformation Eq. (46) (replacing $\mathbf{v}$ by $\mathbf{w}$) leads to the vector equation

$$\mathbf{H}^T\mathbf{w}\{\vartheta;\omega\} = \mathbf{H}^T\mathbf{B}^{-1}\{\vartheta;\omega\}\mathbf{H}\mathbf{A}^{-1}\{\omega\}\mathbf{f}\{\omega\} \tag{49}$$

The matrix $\mathbf{H}$ is a rectangular matrix that has nonzero entries in only n_j columns, and $\mathbf{w}$ is a vector of dimension n_j. Therefore, the corresponding system

$$\mathbf{w}\{\vartheta;\omega\} = \mathbf{B}^{-1}\{\vartheta;\omega\}\mathbf{H}\mathbf{A}^{-1}\{\omega\}\mathbf{f}\{\omega\} \tag{50}$$

is consistent, and a solution of Eq. (50) is equivalent to the solution of Eq. (49). Extracting the term $(1 + \beta_2 j\omega)\mathbf{G}$ from the parenthesis and applying the matrix identity in Eq. (40) yields

$$\mathbf{w}\{\vartheta;\omega\} = (\mathbf{I}_j + (1 + \beta_2 j\omega)\mathbf{G}\{\vartheta\}\mathbf{H}\mathbf{A}^{-1}\{\omega\}\mathbf{H}^T)^{-1}\mathbf{S}\{\vartheta;\omega\} \tag{51}$$

where $\mathbf{I}_j$ is the unity matrix with dimension equal to the number n_j of joint coordinates and the abbreviation

$$\mathbf{S}\{\vartheta;\omega\} = (1 + \beta_2 j\omega)\mathbf{G}\{\vartheta\}\mathbf{H}\mathbf{A}^{-1}\{\omega\}\mathbf{f}\{\omega\} \tag{52}$$

Applying the matrix identity on the term in parenthesis results in

$$\begin{aligned}\mathbf{w}\{\vartheta;\omega\} = (\mathbf{I}_j - (1 + \beta_2 j\omega)\mathbf{G}\{\vartheta\}\mathbf{H}(\mathbf{A}\{\omega\} \\ + \mathbf{H}^T\mathbf{G}\{\vartheta\}\mathbf{H})^{-1}\mathbf{H}^T)\mathbf{S}\{\vartheta;\omega\}\end{aligned} \tag{53}$$

Repeated application of the matrix identity reveals a new set of stochastic basis vectors that are recursively given by

$$\mathbf{w}_0 = \mathbf{G}\{\vartheta\}\mathbf{H}\mathbf{A}^{-1}\{\omega\}\mathbf{f}, \qquad \mathbf{w}_{j+1} = \mathbf{G}\{\vartheta\}\mathbf{H}\mathbf{A}^{-1}\{\omega\}\mathbf{H}^T\mathbf{w}_j \tag{54}$$

The displacement field $\mathbf{w}$ is approximated similar to Eq. (47) as

$$\mathbf{w} \approx \sum_{j=1}^{p} \delta_p \mathbf{w}_p \tag{55}$$

The response statistics are evaluated according to the relations in Eqs. (38) and (39) by applying relation Eq. (46) and replacing $\mathbf{v}$ by $\mathbf{w}$. This method is referred hereto as the second enhanced stochastic reduced basis method (ESRBM2).

IV. Comparison of Calculation Methods

In this section the SRBM, ESRBM1, and ESRBM2 projection schemes are applied to the computation of the response statistics of an example problem with and without damping. Both methods are implemented within the mathematical program environment MATLAB. The system is shown in Fig. 1. The results obtained are benchmarked against those obtained using MCS with a sample size of 1000. Two rectangular plates are clamped on one edge and joined to each other on the opposite edge. The parameters of the deterministic plates and the nondeterministic joint are listed in Table 1. The system is discretized using a mesh of 10×5 and 8×5 thin isotropic plate elements [27], and the joints are modeled by equidistant elastic elements. The stiffness of the line coupling is uncertain, and the Young's modulus Y is expressed by a random field with an assumed spatial correlation. Modelling the Young's modulus by Gaussian variables is not correct physically because it implies a nonzero probability of assigning a negative value to the Young's modulus, which physically must be positive. Nevertheless, for

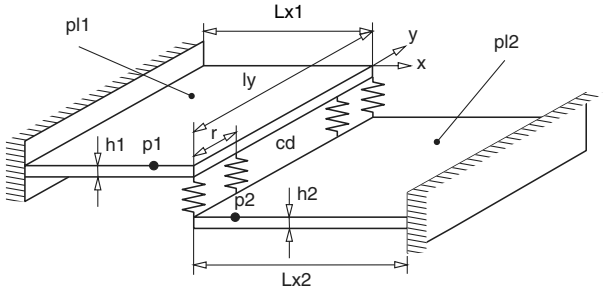

Fig. 1 Plates coupled by a joint with spatially distributed uncertainty.

Table 1 Physical properties and model parameters for the coupled two-plate systems

	ρ, kg/m^3	Y, kN/m^2	ν	L_x, m	L_y, m	h, mm	x elements	y elements
Plate 1	2700	$7 \cdot 10^7$	0.3	$0.5\sqrt{2}$	0.5	3	10	5
Plate 2	2700	$7 \cdot 10^7$	0.3	0.5	0.5	3	8	5
Joint	1350	35 or 50	-	0.006	0.5	3	1	6
Karhunen–Loève expansion		$m = 6$						
Random field (undamped)		$r = L_y/5$		$\sigma = 10\%$			$a = 1000$	
Random field (damped)		$r = L_y/5$		$\sigma = 20\%$			$a = 1000$	
Damping coefficient		$\beta_1 = 0$		$\beta_2 = 5\%$				

sufficiently small values of σ the probability for a negative value is negligible, for example $3 \cdot 10^{-7}\%$ for $\sigma = 20\%$ in Table 1. During the numerical Monte Carlo simulation, the distribution was truncated at $\pm 4\sigma$ in order to avoid negative values for Y.

The system without damping is analyzed first, that is, $\beta_1 = 0 = \beta_2$. A typical frequency response between the points P1 and P2 in Fig. 1 is shown in Fig. 2a. The baseline system is plotted together with the 99.7% (accounts for $\pm 3\sigma$) percentiles of the system responses calculated by MCS with 1000 samples. The frequency range of interest covers the first 12 modes of the structure.

The calculation time of one sample of the direct MCS is compared with that for the full finite element model (FEM) and the reduced model (CMS). For CMS, the first 15 modes of each plate are kept. The relative calculation times are summarized in Table 2, emphasizing the great advantage of applying CMS in order to reduce the number of interior coordinates of each deterministic component while the constraint coordinates remain.

Direct MCS with CMS is compared in terms of accuracy and computational efficiency with the proposed projection schemes SRBM with CMS, ESRBM1 with CMS, and ESRBM2 with CMS, all employing the preconditioned stochastic Krylov subspace. Because no approximation is made from SRBM to ESRBM1 or ESRBM2 all methods lead to exactly the same results. ESRBM1 and ESRBM2 will be referred to together as ESRBM. The mean values and covariances of the frequency responses calculated by MCS in Fig. 2a are shown in Figs. 2b and 2c, respectively. These frequency distributions are compared with the mean and covariance determined by the complex stochastic basis vectors according to Eqs. (38) and (39) and the Petrov–Galerkin scheme in Eq. (37). The accuracy of SRBM/ESRBM depends on the number of basis vectors considered in Eq. (32) or Eq. (44). The higher the value of p in Eq. (31), the closer the results of SRBM/ESRBM are to those of MCS. In the result shown, the SRBM/ESRBM underestimates the MCS distribution, especially in the frequency ranges where sharp resonance peaks occur. However, for the minimum number $p = 2$ as chosen in this

Table 2 Comparison of calculation times for baseline system at 1000 frequencies

	Matrix size n	Constraint DOF	Relative time
FEM	324	36	100%
CMS	66	36	3%

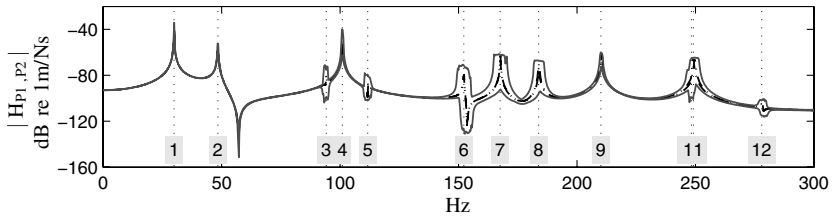

a) Reference transfer mobility for baseline system: full mode and CMS (dashed dot lines) and 99.7% percentiles of MCS with CMS (1000 samples) (solid lines).

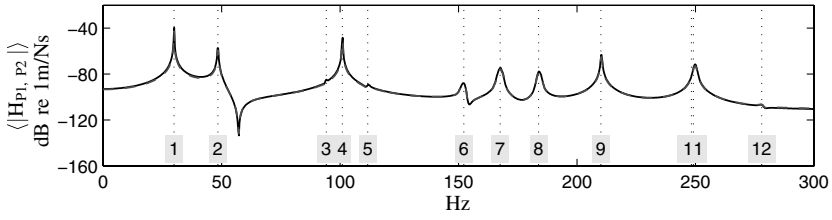

b) Mean transfer mobility for MCS (solid) and SRBM (dashed).

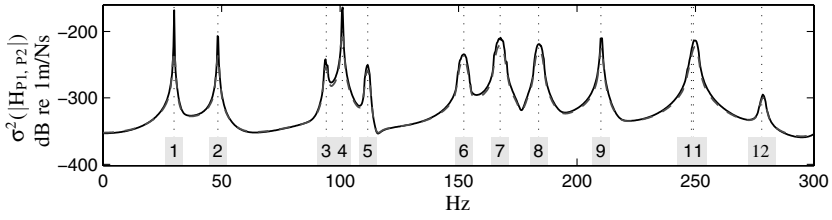

c) First moment of transfer mobility for MCS (solid) and SRBM (dashed).

Fig. 2 Mobility predictions using MCS with CMS and SRBM with CMS for the undamped system.

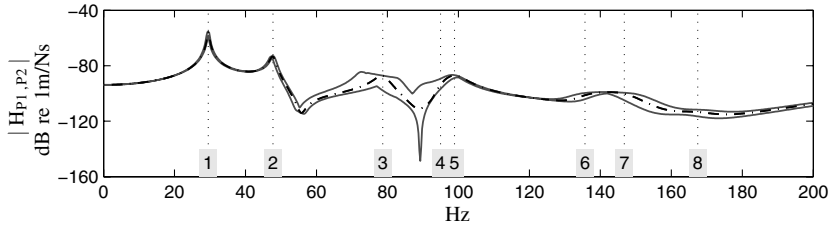

a) Reference transfer mobility for baseline system: full model and CMS (dashed dot lines) and 99.7% percentiles of MCS with CMS (1000 samples) (solid lines).

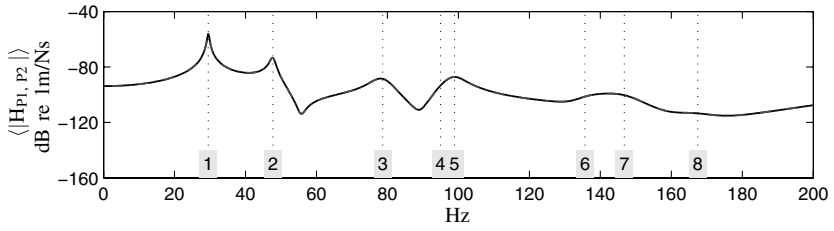

b) Mean transfer mobility for MCS (solid) and SRBM (dashed).

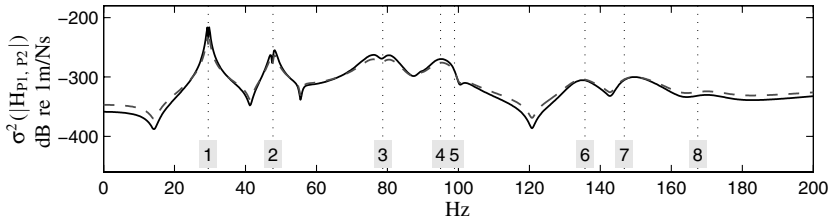

c) First moment of transfer mobility for MCS (solid) and SRBM (dashed).

Fig. 3 Mobility predictions using MCS with CMS (solid) and SRBM with CMS (dashed) for the damped system.

study, leading to a 3×3 coefficient matrix in Eq. (37), the accuracy of the first two statistical moments is good and the characteristics of the distributions are reproduced very well by SRBM/ESRBM.

The system response of the damped system is shown in Fig. 3 with damping coefficients β_1 and β_2 as listed in Table 1. Assuming a frequency independent damping coefficient β_2 results in high loss factors at higher frequencies, see Fig. 3a. Because the resonance peaks of this descriptive example are flattened, the standard deviation σ of the correlation function in Eq. (19) is chosen to be twice as big as in the undamped case. The same comparison is performed as in Fig. 2, but now the underlying stochastic basis vectors are real and the Bubnov–Galerkin scheme is applied by replacing $\mathbf{U}^H$ by $\mathbf{U}^T$ in Eq. (37). Now in the result shown, the SRBM/ESRBM underestimates the MCS distribution in the vicinity of resonance peaks and tends to overestimate the MCS distribution in frequency ranges where antiresonancies occur. Again, for the minimum number $p = 2$ as chosen in this study, the accuracy of the first two statistical moments is good, and the characteristics of the distributions are reproduced very well by SRBM/ESRBM.

The overall calculation times for the undamped and damped cases using CMS are summarized in Table 3, emphasizing the computational efficiency of CMS/SRBM, CMS/ESRBM1, and CMS/ESRBM2. Note that the calculation time of 100% corresponds to the calculation time using CMS, which is itself about 3% of the time of the full FEM solution in Table 2. The significant benefit of the CMS/ESRBM2 scheme compared with CMS/ESRBM1 is due to the smaller number of operations needed for generating the stochastic basis vectors in Eq. (54) compared with Eq. (47).

Table 3 Comparison of calculation times using CMS in Table 2

Method	Relative Time
CMS/MCS with 1000 samples	100%
CMS/SRBM for $p = 2$	36%
CMS/ESRBM1 for $p = 2$	22%
CMS/ESRBM2 for $p = 2$	14%

On one hand, for an MCS the system response is calculated repeatedly over the whole frequency range, and the statistics are obtained by postprocessing. Alternatively, for SRBM/ESRBM these statistics are calculated directly at a fixed frequency, and, consequently, the statistics at each frequency are calculated independently. Hence, the calculation time for MCS strongly depends on the number of samples considered whereas the calculation time for SRBM/ESRBM does not change. So increasing the number of samples for better accuracy of MCS further enhances the relative efficiency of SRBM/ESRBM according to Table 3. The main difference between MCS and SRBM/ESRBM is the type of sampling. Whereas MCS uses samples with respect to the stochastic subspace ϑ, SRBM/ESRBM uses samples with respect to the frequency ω.

V. Conclusions

In this paper different implementations of stochastic reduced basis methods (SRBM) are proposed together with the well-established concept of component mode synthesis (CMS). The efficiencies of these implementations are benchmarked to Monte Carlo simulation (MCS) of a finite element model. For the problem considered, the proposed formulations are efficient and effective implementations of SRBMs. It is seen that SRBMs can be up to orders of magnitude faster than MCS, while providing results of comparable accuracy. Furthermore, the proposed implementations (ESRBM) are more efficient the fewer the number of joints that are affected by uncertainty.

First, a CMS reduction is performed (Craig–Bampton). For each subsystem s the n_i^s fixed-interface modes [Eq. (5)] and the n_b^s static constraint modes [Eq. (6)] are determined and a fraction n_k^s of n_i^s of the fixed-interface modes are kept [Eq. (8)]. Consequently, the finite element model of subsystem s is reduced from its initial size $n_i^s + n_b^s$

to $n_k^s + n_b^s$ [Eq. (10)]. These subsystems are assembled according to Eq. (17), and proportional damping is introduced at this global level [Eq. (18)]. A subsequent global analysis of the deterministic baseline system Eq. (25) is performed, $\mathbf{u}_0$ in Eq. (32). This procedure is evaluated once and is readily available in some commercial software products.

The uncertain parameters in the joints are modeled by random fields that are approximated by a truncated Karhunen–Loève (KL) expansion [Eq. (20)]. Any parameter can be chosen, as long as all system matrices can be approximated by KL expansions similar to Eq. (23). To keep the analysis simple, in the present study a specific correlation function is assumed [Eq. (19)] for the Young's modulus of the joints leading to a variation of the stiffness matrix only [Eq. (23)]. Each joint affected by uncertainty is considered as an individual subsystem/component. This allows the proposed procedures to incorporate joints with complex internal behavior (rubber, foam, etc.) and internal degrees of freedom.

The assembled global system with proportional damping [Eq. (18)] is of size $n = n_b + \sum_s n_i^s$ whereas the reduced global system employing CMS [Eq. (24)] is of size $n_r = n_b + \sum_s n_k^s$, where n_b is the number of linearly independent interface/constraint degrees of freedom ($n_b < \sum_s n_b^s$). In general, the numbers n_k^s of kept internal degrees of freedom of component s are much smaller than the total numbers of internal component degrees of freedom n_i^s. Because the Craig–Bampton CMS is employed no reduction in the number n_b of constraint coordinates is performed.

In the discretization, assembly and solution described previously, various approximation schemes are involved, as well as errors of their expansions due to truncations. In a practical application error and convergence studies might be performed. A commonly accepted guideline for the finite element discretization at component level is that at least six elements per wavelength should be considered. Typically for the CMS models all modes up to twice the highest frequency of interest should be kept. For the Karhunen–Loève expansion in Eq. (23) typically as many terms should be retained to capture 95% of the power (sum of squared values) of the expansion.

In the framework of SRBMs, the displacement vector is approximated by a truncated weighted sum of stochastic eigenvectors [Eq. (31)]. The quality and efficiency of this procedure depends highly on the number and dimension of these vectors. First, the classic definition is reviewed and embedded in the CMS procedure [Eq. (32)]. Then, two different definitions are proposed [Eqs. (44) and (54)]. With these eigenvectors, weighting factors [Eq. (37)] and the statistical moments can be determined [Eqs. (38) and (39)]. Note that the eigenvectors defined in Eqs. (32), (44), and (54) need never to be calculated explicitly, because only their statistics are of interest and not their actual values.

The commonly used definition in Eq. (32) uses vectors of the size of the global system (n or n_r). Much more efficient implementations ESRBM1 and ESRBM2 are derived if the Sherman–Morrison–Woodbury matrix identity Eq. (40) is employed. This leads to new recursive stochastic reduced basis vectors [Eq. (44)] of dimension n_j instead of n or n_r, where n_j is the number of joint degrees of freedom affected by uncertainty and is a fraction of its original size n or n_r in Eq. (32). In the numerical example presented, this reduction in dimension reduces the calculation time relative to the MCS with 1000 samples from 36% for SRBM to 22% for ESRBM1 and 14% ESRBM2. The evaluation of statistical moments in Eqs. (38) and (39) uses recursive definitions of the basis vectors in Eqs. (44) and (50), which employ a repeated multiplication of the same coefficient matrix. This coefficient matrix consists of a sum of two matrices for ESRBM1 and a single matrix for ESRBM2. Determining the first two statistical moments it is sufficient to evaluate only the first three stochastic basis vectors, that is, $p = 2$ in the approximations Eqs. (47) and (55). If $p + 1$ is the number of stochastic basis vectors taken into account, then the number of terms to be evaluated for the second statistical moment [Eq. (39)] is proportional to $(p + 1)^{p+1}$ for ESRBM2 and proportional to $2(p + 1)^{p+1}$ for ESRBM1. Therefore, independent of the number of basis vectors considered, the implementation ESRBM2 is expected to be about a factor of two faster than the implementation ESRBM1.

Acknowledgment

The support of the European Commission within the context of the European Marie Curie Research Training Network (MCRTN) MADUSE (Modelling Product Variability and Data Uncertainty in Structural Dynamics Engineering) is gratefully acknowledged.

References

[1] Melchers, R. E., "Importance Sampling in Structural Systems," *Structural Safety*, Vol. 6, No. 1, 1989, pp. 3–10. doi:10.1016/0167-4730(89)90003-9

[2] Pradlwarter, H. J., and Schuëller, G. I., "On Advanced Monte Carlo Simulation Procedures in Stochastic Structural Dynamics," *International Journal of Non-Linear Mechanics*, Vol. 32, No. 4, 1997, pp. 735–744. doi:10.1016/S0020-7462(96)00091-1

[3] Schuëller, G. I., "Computational Stochastic Mechanics—Recent Advances," *Computers and Structures*, Vol. 79, Nos. 22–25, 2001, pp. 2225–2234. doi:10.1016/S0045-7949(01)00078-5

[4] Schuëller, G. I., "Developments in Stochastic Structural Mechanics," *Archive of Applied Mechanics*, Vol. 75, Nos. 10–12, 2006, pp. 755–773. doi:10.1007/s00419-006-0067-z

[5] Schuëller, G. I., "On the Treatment of Uncertainties in Structural Mechanics and Analysis," *Computers and Structures*, Vol. 85, Nos. 5–6, 2007, pp. 235–243. doi:10.1016/j.compstruc.2006.10.009

[6] Pradlwarter, H. J., Schuëller, G. I., Koutsourelakis, P. S., and Charmpis, D. C., "Application of Line Sampling Simulation Method to Reliability Benchmark Problems," *Structural Safety*, Vol. 29, No. 3, 2007, pp. 208–221. doi:10.1016/j.strusafe.2006.07.009

[7] Liu, W. K., Mani, A., and Belytschko, T., "Finite Element Methods in Probabilistic Mechanics," *Probabilistic Engineering Mechanics*, Vol. 2, No. 4, 1987, pp. 201–213. doi:10.1016/0266-8920(87)90010-5

[8] Mace, B. R., and Shorter, P. J., "A Local Modal/Perturbational Method for Estimating Frequency Response Statistics of Built-Up Structures with Uncertain Properties," *Journal of Sound and Vibration*, Vol. 242, No. 5, 2001, pp. 793–811. doi:10.1006/jsvi.2000.3389

[9] Mace, B. R., Worden, K., and Manson, G., "Uncertainty in Structural Dynamics," *Journal of Sound and Vibration*, Vol. 288, No. 3, 2005, pp. 423–429. doi:10.1016/j.jsv.2005.07.014

[10] Contreras, H., "The Stochastic Finite Element Method," *Computers and Structures*, Vol. 12, No. 3, 1980, pp. 341–348. doi:10.1016/0045-7949(80)90031-0

[11] Yamazaki, F., and Shinozuka, M., "Neumann Expansion for Stochastic Finite Element Analysis," *Journal of Engineering Mechanics*, Vol. 114, No. 8, 1988, pp. 1335–1354. doi:10.1061/(ASCE)0733-9399(1988)114:8(1335)

[12] Ghanem, R., and Spanos, P., *Stochastic Finite Elements: A Spectral Approach*, Springer–Verlag, New York, 1991.

[13] Kleiber, M., and Hien, T. D., *The Stochastic Finite Element Method*, Wiley, New York, 1992.

[14] Nair, P. B., and Keane, A. J., "Stochastic Reduced Basis Methods," *AIAA Journal*, Vol. 40, No. 8, 2002, pp. 1653–1664. doi:10.2514/2.1837

[15] Hurty, W. C., "Dynamic Analysis of Structural Systems Using Component Modes," *AIAA Journal*, Vol. 3, No. 4, 1965, pp. 678–685. doi:10.2514/3.2947

[16] Craig, R. R., and Bampton, M., "Coupling of Substructures for Dynamic Analysis," *AIAA Journal*, Vol. 6, No. 7, 1968, pp. 1313–1319. doi:10.2514/3.4741

[17] Karhunen, K., "Über Lineare Methoden in der Wahrscheinlichkeitsrechnung," *Annales Academiae Scientiarum Fennicae. Series A. I, Mathematica*, Vol. 37, 1947, pp. 3–79.

[18] Vanmarcke, E., *Random Fields Analysis and Synthesis*, MIT Press, Cambridge, MA, 1988.

[19] Zeldin, B. A., and Spanos, P. D., "On Random Field Discretization in Stochastic Finite Elements," *Journal of Applied Mechanics*, Vol. 65, No. 2, 1998, pp. 320–327. doi:10.1115/1.2789057

[20] Dohnal, F., Mace, B. R., and Ferguson, N. S., "Modelling Uncertainty in Joints Using Component Mode Synthesis and a Stochastic Reduced Basis Method," *Proceedings of EUROSIM*, ARGESIMedited

by B. Zupanèiè, R. Karba, and S. Blažiè, 2007.
[21] Dohnal, F., Mace, B. R., and Ferguson, N. S., "Analysis of Vibrations of Systems with Spatially Correlated Uncertainty in Joints Using a Stochastic Reduced Basis Method," *7th European Conference on Structural Dynamics (EURODYN)*, Paper E311 [CD-ROM], 2008.
[22] Craig, R. R., Jr., *Structural Dynamics—An Introduction to Computer Methods*, Wiley, New York, 1981.
[23] Guyan, R. J., "Reduction of Stiffness and Mass Matrices," *AIAA Journal*, Vol. 3, No. 2, 1965, p. 380. doi:10.2514/3.2874
[24] Field, R. V., and Grigoriu, M., "On the Accuracy of the Polynomial Chaos Approximation," *Probabilistic Engineering Mechanics*, Vol. 19, Nos. 1–2, 2004, pp. 65–80. doi:10.1016/j.probengmech.2003.11.017
[25] Kirsch, U., "Reduced Basis Approximation of Structural Displacements for Optimal Design," *AIAA Journal*, Vol. 29, No. 10, 1991, pp. 1751–1758. doi:10.2514/3.10799
[26] Golub, G. H., and Van Loan, C. F., *Matrix Computations*, 2nd ed., Johns Hopkins Univ. Press, Baltimore, MD, 1989.
[27] Petyt, M., *Introduction to Finite Element Vibration Analysis*, Cambridge Univ. Press, Cambridge, England, UK, 1990.

A. Messac
Associate Editor